Discrimination between Internal Waves and Temperature Finestructure

TERRENCE M. JOYCE

Woods Hole Oceanographic Institution, Woods Hole, Mass. 02543

YVES J. F. DESAUBIES

Applied Physics Laboratory, University of Washington, Seattle, 98105

(Manuscript received 1 December 1975, in revised form 23 August 1976)

ABSTRACT

Discrimination between internal waves and finestructure in the ocean is made difficult because of overlapping scales of each process. We have assumed as a working hypothesis that low frequency/wavenumber variability is predominantly wave-like, while high frequency/wavenumber variability is step-like. Thermal finestructure is modeled as a steppy Poisson process in the vertical, while internal waves are modeled as a random Gaussian process. The model developed is an extension of one of McKean (1974). We describe the vertical temperature spectrum of finestructure, and moored temperature and temperature difference measurements of the internal wave experiment (IWEX). For the data considered, the contamination of moored spectra and cross-spectra is small for low frequencies. The vertical temperature difference, measured over a vertical distance which is small compared to the correlation length of the internal wave field, is shown to provide a critical check of the model, since this signal is directly related to finestructure variability. Thus, it appears possible to use moored differential temperature sensors as monitors of finestructure activity.

1. Introduction

The small-scale vertical temperature structure in the oceans is highly irregular and often consists of small-scale regions of uniform temperature on the order of meters or tens of meters separated by regions of rapid changes in temperature. These scales of variability have been named finestructure and have been the subject of study for over 15 years. Internal waves displace this structure vertically as well as contribute to the signal by straining the existing thermal field. Those interested in the measurement of internal gravity waves have tried to infer vertical displacements at a point in the ocean by the relation

$$\zeta = -\left(\frac{\overline{\partial T}}{\partial y}\right)^{-1} T',$$

where y is the vertical coordinate, T is temperature, T' is temperature anomaly and the overbar denotes some "appropriate" average. In the presence of a highly irregular temperature structure, the validity of this approximation is not always clear. It was first pointed out by Phillips (1971) that the use of the above method would induce errors in the inferred internal wave field. Others (Reid, 1971; Garrett and Munk, 1971; McKean, 1974) have also found that the temperature frequency spectrum can be expressed as the sum of two terms: a "gradient spectrum" simply related to the mean temperature gradient and a finestructure spectrum proportional to the inverse square of the frequency.

Assuming the finestructure to be statistically stationary in depth and the vertical displacement jointly normal, Garrett and Munk (1971) derive an integral relation between the finestructure spectrum and the vertical wavenumber spectrum of the finestructure. One difficulty in utilizing their model is the inability to distinguish the purely passive finestructure component from the straining due to internal waves in the vertical spectra of temperature, especially when vertical temperature spectra were consistent with the supposition that the variability was due to high mode number internal waves (Garrett and Munk, 1975; Hayes *et al.*, 1975). A new approach to the problem was made by McKean (1974), who modeled that portion of the thermal field which is characterized as sheets and layers and then studied its effect upon the measurements of internal gravity waves.

In this paper we will use and extend the formalism suggested by McKean. The finestructure parameters are obtained from several CTD casts and are shown to be well represented by a vertical Poisson process. The model is then applied to moored temperature data from the internal wave experiment (IWEX). The theory is also extended to model temperature difference time series and vertical temperature spectra. Before proceeding we will for completeness define some of the statistical quantities soon to be discussed.

For a stationary random variable $x_1(t)$ with zero mean, the covariance γ, frequency spectrum P, and structure function D are defined and related as follows:

$$\left.\begin{aligned}\gamma_{11}(\tau)&=\langle x_1(t+\tau)x_1(t)\rangle\\&=\int_0^\infty P_{11}(f)\cos 2\pi f\tau df\\P_{11}(f)&=4\int_0^\infty \gamma_{11}(\tau)\cos 2\pi f\tau d\tau\\D_{11}(\tau)&=\langle[x_1(t+\tau)-x_1(t)]^2\rangle\\&=2\int_0^\infty P_{11}(f)[1-\cos 2\pi ft]df\end{aligned}\right\}. \quad (1)$$

The brackets $\langle\ \rangle$ denote an ensemble average.

2. Theoretical models

The temperature profile is represented locally as a superposition of homogeneous layers of thickness z_i with temperature jump θ_i across the interfaces.

The temperature difference over a vertical interval Δ containing N layers is

$$\left.\begin{aligned}\Delta T&=t'\Delta+\sum_{i=1}^{N}\theta_i\\\langle\Delta T\rangle&=\alpha\Delta,\quad \alpha\equiv t'+\mu\langle\theta\rangle\end{aligned}\right\}, \quad (2)$$

where t' is a residual gradient, while the probability of finding N steps over the distance Δ is given by the Poisson distribution

$$p(N,s)=e^{-s}\frac{s^N}{N!},\quad s=\mu\Delta, \quad (3)$$

where μ^{-1} is the average layer thickness. We extend the result of McKean to allow covariance between adjacent temperature steps.

a. *Moored temperature measurements*

The vertical displacements of the internal wave field are stationary and jointly normal with variance Z^2 and autocorrelation function $\rho(\tau)$. For measurements at a fixed point, McKean (1974) introduced a structure function that is more appropriate than the correlation function. The temperature spectrum is then found to be the sum of two terms (Garret and Munk, 1971)

$$P^T(f)=\bar{P}^T(f)+P^{TF}(f),\quad \bar{P}^T(f)\equiv\alpha^2P^z(f). \quad (4)$$

The first term, the gradient spectrum $\bar{P}^T$, is related to the mean temperature gradient α; the second is the finestructure spectrum. For a displacement spectrum of the form

$$P^z(f)=Af^{-2}, \quad (5)$$

two approximations are obtained for P^{TF}:

$$P_-^{TF}=\beta A^{\frac{1}{2}}f^{-\frac{1}{2}}/(2\pi^{\frac{1}{2}}),\quad f<n, \quad (6)$$

$$P_+^{TF}=\beta ZSf^{-2}/(2\pi^5)^{\frac{1}{2}},\quad f>n, \quad (7)$$

where $\beta=\mu[\langle\theta^2\rangle+2\,\mathrm{cov}(\theta_i,\theta_j)]$. In these expressions $\langle\theta^2\rangle$ is the mean-square temperature jump across the layers, $\mathrm{cov}(\theta_i,\theta_j)$ is the covariance between temperature jumps i, j for $i\neq j$, n is the local bouyancy frequency and

$$S^2=-\frac{\rho''(0)}{\rho(0)}, \quad (8)$$

so that ZS is the root-mean-square (rms) vertical velocity of the internal waves.

For cross spectra of measurements taken at two points i and j, one writes as in (4),

$$P_{ij}^T(f)=\bar{P}_{ij}^T+P_{ij}^{TF}, \quad (9)$$

and the coherence R_{ij}^T is defined as the modulus of the quotient of P_{ij}^T by $(P_{ii}^TP_{jj}^T)^{\frac{1}{2}}$, i.e.,

$$R_{ij}^T(f)=\left|\frac{\bar{C}_{ij}^T+rC_{ij}^{TF}}{1+r}\right|. \quad (10)$$

The notation is as follows:

$$\bar{C}_{ij}^T\equiv\bar{P}_{ij}^T/(\bar{P}_{ii}^T\bar{P}_{jj}^T)^{\frac{1}{2}} \quad (11)$$

is the normalized gradient cross spectrum, and

$$C_{ij}^{TF}\equiv P_{ij}^{TF}/(P_{ii}^{TF}P_{jj}^{TF})^{\frac{1}{2}} \quad (12a)$$

is the normalized finestructure cross spectrum. It has been called the finestructure coherence (denoted Λ) by Garrett and Munk, a somewhat misleading appelation since C_{ij}^{TF} could, *a priori*, be complex, whose real part will turn out to take positive and negative values. Finally

$$r\equiv P_{ii}^{TF}/\bar{P}_{ii}^T=P_{jj}^{TF}/\bar{P}_{jj}^T \quad (12b)$$

is the finestructure ratio.

For sensors vertically separated by Δ, McKean (1974) gave

$$C_{ij}^{TF}=e^{-t}(\cos t+\sin t),\quad t=(f/\pi A)^{\frac{1}{2}}\Delta,\quad f<n, \quad (13)$$

$$C_{ij}^{TF}=2\int_0^\infty \exp(-u^2)u^{-3}\cos\lambda u du,\qquad \lambda=\sqrt{2}\pi f\Delta/ZS,\quad f>n, \quad (14)$$

the last expression being Garrett and Munk's "finestructure coherence."

b. *The temperature difference measurements*

During Woods Hole Oceanographic Institution's internal wave experiment (IWEX), a number of sensors recorded directly the temperature difference ΔT over a vertical separation $\Delta=1.74$ m. We shall show

that these measurements provide an estimate of the finestructure activity.

1) THE SPECTRUM OF ΔT

Consider two sensors at points 1 and 2, vertically separated by Δ; let $\Delta T \equiv T_2 - T_1$. The spectrum of the difference temperature $P^{\Delta T}(f)$ is

$$P^{\Delta T}(f) = 4\int_0^\infty \gamma^{\Delta T}(\tau)\cos 2\pi f\tau d\tau, \tag{15}$$

where $\gamma^{\Delta T}(\tau) \equiv \langle \Delta T(t)\Delta T(t+\tau)\rangle$ is the temperature difference covariance function. We have

$$\begin{aligned}\gamma^{\Delta T} &= \langle (T_2T_2' + T_1T_1' - T_2T_1' - T_1T_2')\rangle \\ &= \gamma_{22}^T + \gamma_{11}^T - 2\gamma_{12}^T,\end{aligned} \tag{16}$$

where the prime implies evaluation at $t+\tau$. For small enough separations (over which the ocean can be considered homogeneous), after taking the Fourier transform, we then obtain

$$P^{\Delta T}(f) = 2P^T - 2P_{12}^T. \tag{17}$$

Substituting (4) and (9) into (17), we finally have

$$P^{\Delta T}(f) = 2\bar{P}^{TF}(1-\bar{C}_{12}^T) + 2P^{TF}(1-C_{12}^{TF}), \tag{18}$$

where P^{TF} and C_{12}^{TF} are given by (6), (7), (13) and (14). The spectrum of the temperature difference signal is thus the sum of internal wave and finestructure contributions.

2) CROSS SPECTRA OF ΔT

We consider now two ΔT pairs of sensors, vertically separated by Y. The cross spectrum of the ΔT signal is another measure of the finestructure field and provides a further check of the model. The four sensors aligned vertically are located at y_1, y_2, y_3, y_4 from the bottom up, with separations $y_2 - y_1 = y_4 - y_3 = \Delta$ and $y_4 - y_2 = y_3 - y_1 = Y$; the pair 1, 2 is denoted by i; 3, 4 by j.

The cross spectrum $P_{ij}^{\Delta T}(y,f)$ is the transform of the cross-covariance function

$$\begin{aligned}\gamma_{ij}^{\Delta T}(\tau) &= \langle \Delta T_i(t)\Delta T_j(t+\tau)\rangle \\ &= \langle (T_2 - T_1)(T_4' - T_3')\rangle \\ &= \langle (T_2T_4' + T_1T_3' - T_1T_4' - T_2T_3')\rangle\end{aligned} \tag{19}$$

and is

$$P_{ij}^{\Delta T}(Y,f) = P_{24}^T + P_{13}^T - P_{14}^T - P_{23}^T. \tag{20}$$

Based essentially on the model of Garrett and Munk (1975), Cairns and Williams (1976) and Desaubies (1976) have shown that the internal wave normalized cross spectrum can be written

$$\bar{C}_{ij}^T = \exp[-2\pi q n(y_i - y_j)]$$

(q is a constant). For the small separations Y and Δ we shall be concerned with here, the exponential can be approximated by a linear function of separation and we have $\bar{P}_{24}^T + \bar{P}_{13}^T - \bar{P}_{14}^T - \bar{P}_{23}^T = 0$, so that only the finestructure contributions remain in (20). Dividing through by (18), we have for the coherence

$$R^{\Delta T}(Y,f) = \left| \frac{2C^{TF}(Y) - C^{TF}(Y-\Delta) - C^{TF}(Y+\Delta)}{2[1-C^{TF}(\Delta)]} \right|, \tag{21}$$

where the C^{TF}'s are the normalized finestructure cross spectra defined in (12) with the separation shown as the argument.

c. Vertical spectra

In a manner similar to that employed for moored spectra, vertical or dropped spectra can also be calculated from the parameters available. To eventually derive vertical spectra it will be necessary to eliminate from the temperature structure function contributions arising from nonzero mean values for the temperature.

$$\begin{aligned}D^T(Y) = \langle \{ &[T(y+Y,t) - \bar{T}(y+Y,t)] \\ &- [T(y,t) - \bar{T}(y,t)]\}^2\rangle.\end{aligned} \tag{22}$$

Averaging over the random steps gives

$$\left.\begin{aligned} D^T(Y) &= \alpha^2\langle(\zeta_2 - \zeta_1)^2\rangle + \langle |Y + \zeta_2 - \zeta_1|\rangle \\ \zeta_2 &= \zeta(y+Y,t) \\ \zeta_1 &= \zeta(y,t)\end{aligned}\right\}. \tag{23}$$

The brackets in (23) denote ensemble averaging over the internal wave field.

$$\left.\begin{aligned} \langle (Y + \zeta_2 - \zeta_1)^n\rangle &= \int_{-\infty}^{\infty} du p(u,Y)(Y+u)^n \\ u &\equiv \zeta_2 - \zeta_1\end{aligned}\right\}. \tag{24}$$

For a jointly normal homogeneous internal wave field,

$$p(u,Y) = \frac{1}{\sigma\sqrt{2\pi}}\exp\left(-\frac{u^2}{2\sigma^2}\right),$$

$$\sigma^2 = 2Z^2[1-\rho(Y)].$$

The first term in (23) is the mean gradient term and is solely due to internal waves, while the second is the finestructure term. Vertical structure functions differ from moored or horizontal ones in that the signature of the sheets and layers will be present in the total absence of internal waves.

$$D^{TF}(Y|u=0) = \beta Y, \quad \beta \equiv (\overline{\theta^2} + 2\,\mathrm{cov}\theta)\mu. \tag{25}$$

The vertical spectrum of finestructure $P^{TF}(k)$ will be proportional to k^{-2}. Furthermore it will have no low wavenumber cutoff (since the Poisson process is aperiodic). The necessity to have but the inability to measure a *largest* scale of finestructure was a major difficulty of earlier papers using spectral models.

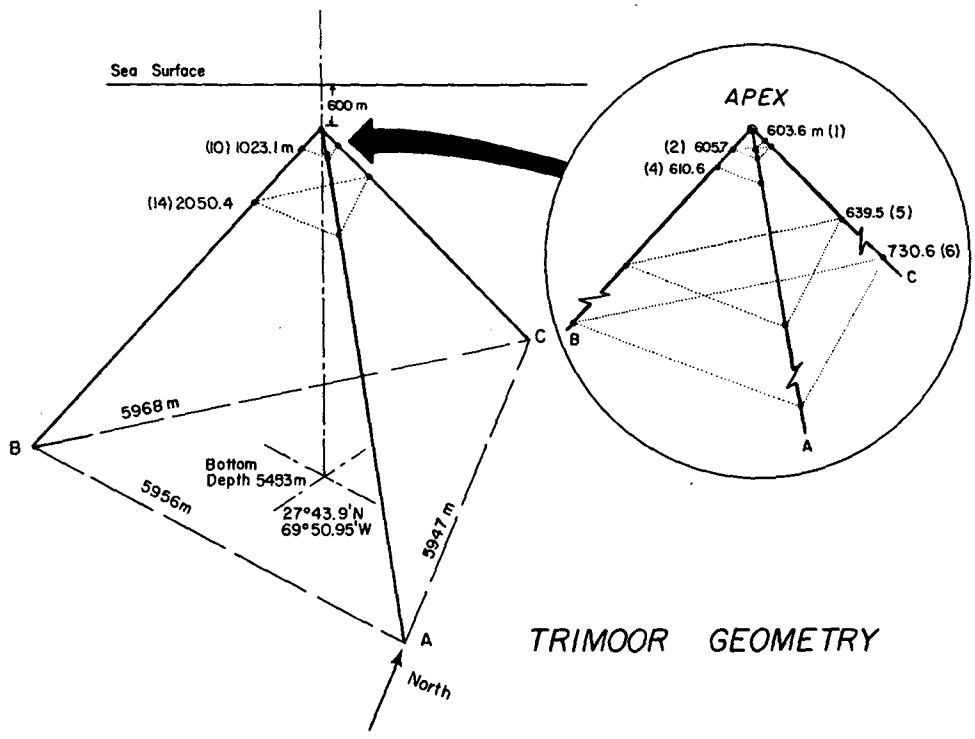

FIG. 1. Schematic of the internal wave experiment (TWEX) Trimoor.

In the presence of internal waves and finestructure the contribution in (23) can be evaluated as follows:

$$D^{TF}(Y)$$

$$=\beta\int_{-\infty}^{\infty} du\,p(u,Y)|u+Y|$$

$$=\beta\int_{-\infty}^{Y} du\,p(u,Y)(-u-Y)+\beta\int_{-Y}^{\infty} du\,p(u,Y)(u+Y)$$

$$=\beta\int_{-\infty}^{\infty} du\,p(u,Y)(u+Y)-2\beta\int_{-\infty}^{Y} du\,p(u+Y)(u+Y)$$

$$=\beta\left\{Y\,\mathrm{erf}\left(\frac{Y}{\sigma\sqrt{2}}\right)+\sqrt{2/\pi}\sigma\exp\left(-\frac{Y^2}{2\sigma^2}\right)\right\}. \tag{26}$$

Together with an internal wave model for $\rho(Y)$, this constitutes a formal solution to the calculation of vertical spectra. We will examine two particular limits $(Y/\sigma\sqrt{2})\gg 1, \ll 1$.

For $(Y/\sigma\sqrt{2})\gg 1$

$$D^{TF}(Y)=\beta Y, \tag{27}$$

$$P^{TF}(k)=\beta/(2\pi^2k^2). \tag{28}$$

For $(Y/\sigma\sqrt{2})\ll 1$

$$D^{TF}(Y)=\sqrt{2/\pi}\beta\sigma$$
$$=\sqrt{2/\pi}\beta\sqrt{D_\zeta(Y)}. \tag{29}$$

If the internal wave vertical spectrum $P^\zeta(k)$ is proportional to k^{-t}, then the finestructure spectrum is proportional to k^{-q}, with $q=1+(t-1)/2$, for $1<q<3$.

These two limits correspond respectively to wavelengths much larger than or smaller than the rms vertical displacement of the isotherms Z. The former limit corresponds exactly to the result for no internal waves, while the latter limit may in fact be nonphysical, since it applies to vertical scales of tens of centimeters. The model for the finestructure is nonphysical on these smaller scales: it predicts an infinite variance to the temperature gradient when in fact the transitions from one layer to the next have finite thicknesses of the order of tens of centimeters. We will further consider only the former limit given by (28).

3. Data base

The data used in this study were collected in the Sargasso Sea of the northwest Atlantic Ocean and include both moored and vertically profiling measurements. The basic moored data were obtained during the internal wave experiment (IWEX) from a highly stable subsurface trimooring shown in Fig. 1. The upper main thermocline (600–800 m) was highly instrumented with vector averaging current meters modified to measure temperature as well as vertical temperature difference over one instrument length (1.74 m). A full discussion of the IWEX experiment can be found in Briscoe (1975).

Vertical profiles of temperature and salinity were taken with the WHOI/Brown CTD unit. Six "typical" stations were selected for subsequent analysis. These were located in the vicinity of the trimoor and are

TABLE 1. Sample CTD stations selected for estimation of finestructure statistics in the main thermocline, 600–800 db.

Station	Latitude	Longitude	Date
CH107/08	27°33.9N	69°44.8W	10/31/72
CH107/17	27°33.7N	69°41.8W	11/03/72
CH112/148	28°00.9N	69°35.7W	8/04/73
KN34/09	27°45.1N	69°49.1W	10/25/73
KN34/13	27°45.3N	69°52.5W	10/28/73
KN34/16	27°46.2N	69°51.0W	10/31/73
IWEX	27°43.9N	69°51.0W	11/04/73–12/13/73

lisited in Table 1. The list includes stations near the IWEX site over a two-year period. The natural variability of finestructure with vertical and horizontal locations in the Sargasso Sea has been described by Hayes *et al.* (1975) and Joyce (1976), respectively. For comparison with the IWEX data, only a portion of the main thermocline (600–800 m) was selected for modeling of the statistical structure of the temperature field. For vertical scales as small as 2 m in this region Joyce (1976) showed that the temperature and salinity fields are well correlated and that variations in temperature are statistically the same as density. Instrument limitations preclude study of smaller scales in the thermocline.

4. Statistical model of finestructure

It has been observed that much of the small-scale structure of the temperature/salinity field in the ocean can be characterized as layers (regions of relatively mixed water) and sheets (regions of large vertical gradients). Gregg (1975) has coined the phrase "irregular steppy" to describe this phenomenon. An example of the vertical temperature gradient from CTD station 17 seen in Fig. 2 depicts the "irregular steppy" nature of the thermal field on scales in excess of 30 cm. Vertical spectra of the temperature field are easily calculated and tend to be "red" with a power law dependence k^{-n} on wavenumber with n approximately 2.6 for scales between 50 and 0.5 m. We will, however, utilize the original traces of temperature versus depth (or pressure) to construct a statistical model for the finestructure steps. The resulting profile will reproduce the step-like phenomena but not necessarily the vertical spectrum.

The temperature difference θ_i between the i and $i+1$ steps is a random variable as is the thickness of the ith step Z_i. The manner in which θ_i and Z_i are found in a CTD profile is most easily described by reference to Fig. 2. The differenced series shown can be thought of as consisting of events (temperature jumps) occurring randomly in space with a random amplitude. To find such an event in a temperature series it is only necessary to locate local maximum of the differenced series. The values of the maxima yield the θ_i, while the distances between successive maxima give the Z_i's. In an observed profile, account must be taken of any noise in the system as it will obviate the detection scheme.

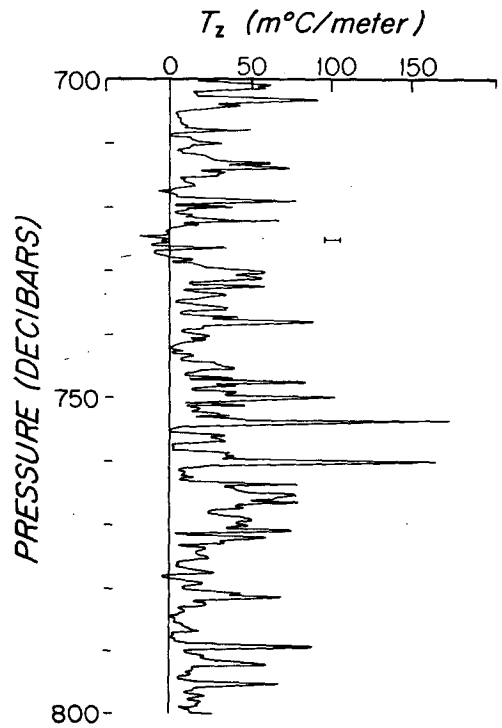

FIG. 2. Vertical temperature gradient in the main thermocline of the Sargasso Sea. Differencing interval is 30 cm; uncertainty due to instrumental noise is indicated. The data are from CTD Station CH 107/17.

The rms noise level of the lag-corrected pressure-sorted CTD temperature series used was 10^{-3} °C or 0.003% full scale of the instrument (~30°C). For a first differenced series which has been decimated to a data point every 30 cm, we estimate the noise level to be approximately 0.8 m °C. Events were selected, therefore, only when the local maximum of the differenced series exceeded neighboring values by some noise limit. For random Gaussian noise a limit of 1 m °C would encompass 80% of the possible noise values. Sensitivity tests to imposed noise limits of 0% (all noise allowed to pass) and 99% (2 m °C noise) were made as well. Larger noise limits effectively filter out small θ_i and Z_i; thus a compromise was necessary. Further discussion of this will follow.

From the desired series θ_i, Z_i, first and second order moments were calculated. $\langle\theta_i\rangle$, $\langle Z_i\rangle$, $\mathrm{var}\theta_i$, $\mathrm{var}Z_i$, $\mathrm{cov}(\theta_i,\theta_j)$, $\mathrm{cov}(Z_i,Z_j)$ and $\mathrm{cov}(\theta_i,Z_i)$. An ensemble average of all six stations was taken and the results

TABLE 2. Results from analysis of stations in Table 1 using a noise level of 1 m °C. Over 700 "events" are included in this summary.

$\langle Z_i\rangle$ (m)	$\mathrm{var}Z_i$ (m)²	$\mathrm{cov}(Z_i,Z_j)$ (m)²	$\langle\theta_i\rangle$ (m °C)	$\mathrm{var}\theta_i$ (m °C)²	$\mathrm{cov}(\theta_i,\theta_j)$ (m °C)²	$\mathrm{cov}(\theta_i,Z_i)$ (m °C·m)
1.65 m	1.18	0	11.85	45.6	4.56	0

summarized in Table 2 and Figs. 3 and 4. A noise limit of 1 m °C was used.

From these it can be seen that to second order, θ_i and Z_i are independent and that each step Z_i is independent of its neighbors. Both of these results are consistent with the Poisson model discussed earlier. The histograms of both θ_i and Z_i are highly skewed. For a Poisson process, the probability of encountering N steps in a vertical distance Δ is given by Eq. (3). The probability density function for the step thickness $p(Z_i)$ can be expressed

$$p(Z_i)=\mu \exp(-\mu Z_i). \tag{30}$$

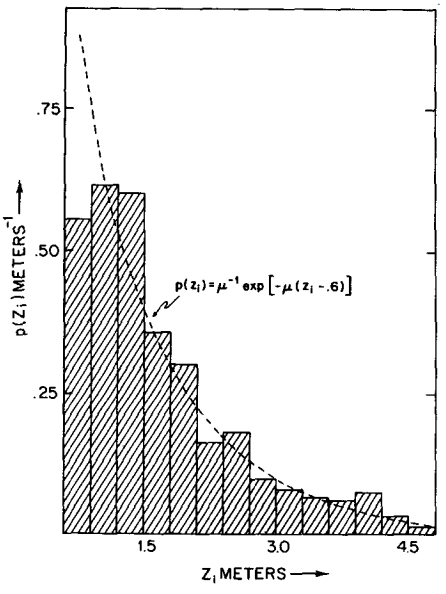

(a)

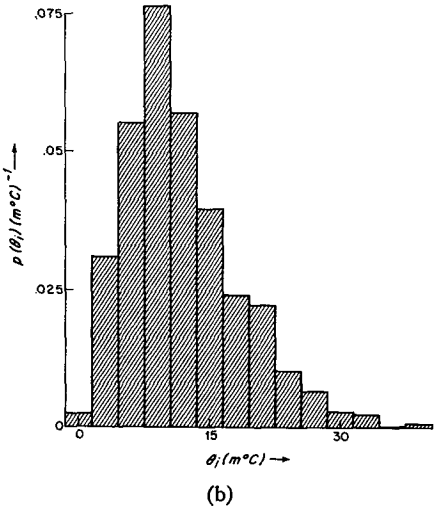

(b)

FIG. 3. Probability histograms for (a) step size and (b) temperature jumps. Also shown in (a) is the analytical relation (34).

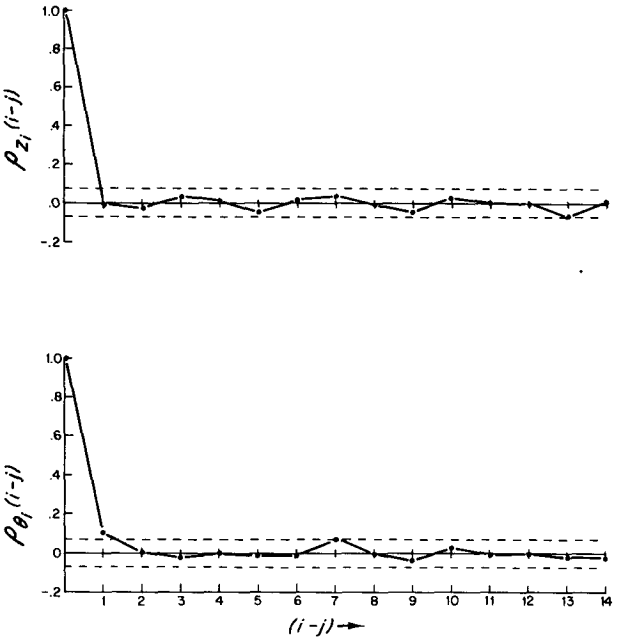

FIG. 4. Autocorrelation coefficients for step size Z_i and temperature jump θ_i. Ninety-five percent confidence limits are indicated.

Hence

$$\langle Z_i\rangle=\int_0^\infty Z_i p(Z_i)dZ_i, \tag{31}$$

$$\text{var}Z_i=\int Z_i^2 p(Z_i)dZ_i-\langle Z_i\rangle^2. \tag{32}$$

Since we cannot measure $Z_i \lesssim Z_L=0.6$ m, the probability density function $p(Z_i)$ must be renormalized to be $\hat{p}(Z_i)$ so that

$$\int_0^\infty p(Z_i)dZ_i=\int_{Z_L}^\infty \hat{p}(Z_i)dZ_i=1. \tag{33}$$

Thus

$$\hat{p}(Z_i)=\mu \exp[-\mu(Z_i-Z_L)], \tag{34}$$

$$\langle Z_i\rangle=\int_{Z_L}^\infty Z_i\hat{p}(Z_i)dZ_i=Z_L+\mu^{-1}, \tag{35}$$

$$\text{var}Z_i=\int Z_i^2\hat{p}(Z_i)dZ_i-(Z_L+\mu^{-1})^2=\mu^{-2}. \tag{36}$$

In order to apply the model of finestructure to moored and dropped measurements the only further parameter necessary to extract from the data is the mean rate of occurrence of "events" μ. This can be done by using (34), (35) or (36), since all of these equations only depend upon μ. We find

$$\mu=0.92 \text{ (m)}^{-1} \text{ using (35)},$$
$$\mu=0.95 \text{ (m)}^{-1} \text{ using (36)}.$$

TABLE 3. Sensitivity of parameters of Table 2 to different noise limits for one of the six CTD stations.

Noise limit	μ $(m)^{-1}$	$\bar{\theta}$ (m °C)	varθ (m °C)^2	cov(θ) (m °C)^2	β (m °C$^2\cdot$m^{-1})
0 m °C	2.28	10.0	43.4	12.2	382
1 m °C	1.01	10.2	41.5	4.2	154
2 m °C	0.52	13.8	39.8	0	120

In Fig. 3 are shown the analytical relation (34) and the observed distribution of step size. The data/model fit is evidently self-consistent.

As was shown earlier, the intensity of the finestructure signal is proportional to

$$\beta\equiv\mu[\langle\theta^2\rangle+2\,\mathrm{cov}(\theta_i,\theta_j)].$$

The sensitivity of the individual parameters and the above intensity to different noise limits are shown in Table 3 for one of the six stations. It is clear from the table that the values of the individual parameters are sensitive to the limits. The intensity, however, does not strongly depend upon the particular choice of either 1 or 2 m °C noise. We expect our estimates of the finestructure intensity, which will be used subsequently, to be correct to within 20%.

5. Results

The finestructure parameters have been obtained in Section 4. In determining these values from CTD profiles, it has been implicitly assumed that the small-scale thermal structure was only slightly distorted by internal wave straining. Similarly, the internal wave parameters appearing in the model will now be derived from the observed temperature spectra, an appropriate procedure only if the finestructure contamination is small. Our results will have to be checked *a posteriori* to verify these assumptions. From Table 2 we obtain for the finestructure intensity $\beta=1.81\times10^{-4}$ (°C)^2 m^{-1}. The displacement spectrum [Eq. (5)] is related to the temperature spectrum through the mean temperature gradient α:

$$P^\zeta(f)=Af^{-2}=\alpha^{-2}\bar{P}^T(f)=\alpha^{-2}Bf^{-2}. \qquad (37)$$

The constant B is obtained by fitting the f^{-2} law to the observed spectrum so as to preserve the variance of the signal. We find $B=5.96\times10^{-4}$ (°C)^2 cph, and, with the observed $\alpha=0.01768$ (°C m^{-1}), $A=1.91$ m^2 cph. The rms displacement

$$Z=\left[A\int_{f_i}^{n}f^{-2}df\right]^{\frac{1}{2}}\approx[Af_i^{-1}]^{\frac{1}{2}}=6.90\text{ m} \qquad (38)$$

and the quantity S, defined in (8), is

$$S^2=-\rho''(0)/\rho(0)=4\pi^2Z^{-2}\int_{f_i}^{n}f^2P^\zeta(f)df$$
$$\approx4\pi^2nf_i=(2.00\text{ cph})^2, \qquad (39)$$

where $n=2.52$ cph is the local Väisälä frequency at 604 m and $f_i=0.04$ cph is the local inertial frequency.

6. Moored temperature measurements

The finestructure spectrum P^{TF}, given by (6) and (7), is compared to the gradient spectrum $\bar{P}^T=\alpha^2P^\zeta$ in Fig. 5. Over the internal wave frequency band, P^{TF} is about one-tenth of $\bar{P}^T$; at higher frequencies ($f>n$) the finestructure spectrum is smaller than but comparable to the tail of $\bar{P}^T$. Because of the two approximations [(6) and (7)] there is a discontinuity at $f=n$. The finestructure contamination is small in the internal wave band, a 10% effect, while above the buoyancy cutoff the finestructure is a significant contribution to the observed temperature spectrum. Thus the finestructure contamination is small, in the range $f_i<f<n$, and moored temperature observations are an appropriate measure of internal waves.

An estimate of the effect of finestructure on moored vertical coherence can be derived from (10). The normalized internal wave cross spectrum $\bar{C}^T$ is given by

$$\bar{C}^T_{ij}=\pm R^T_{ij}(1+r)-rC^{TF}_{ij}, \qquad (40)$$

where R^T_{ij} is the observed coherence, C^{TF}_{ij} is given by (13) and (14), and the finestructure ratio r [Eq.

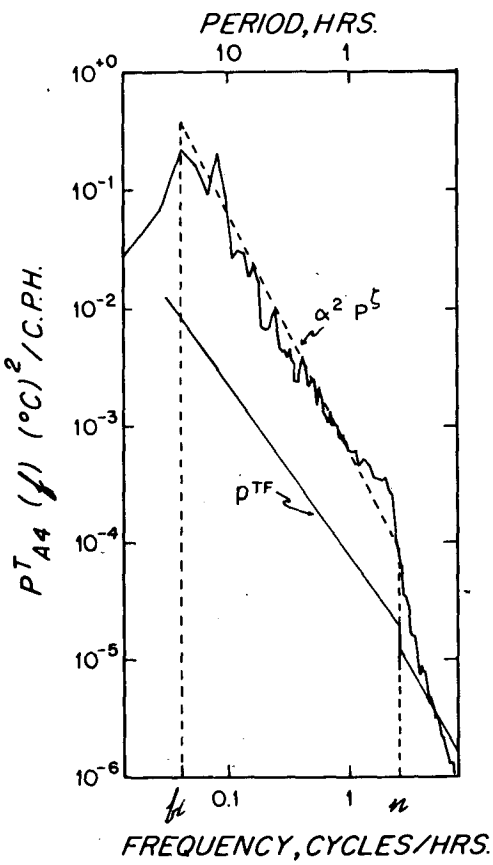

FIG. 5. Observed temperature frequency spectrum from IWEX instrument A4, $P^T_{A4}(f)$ and model results from text.

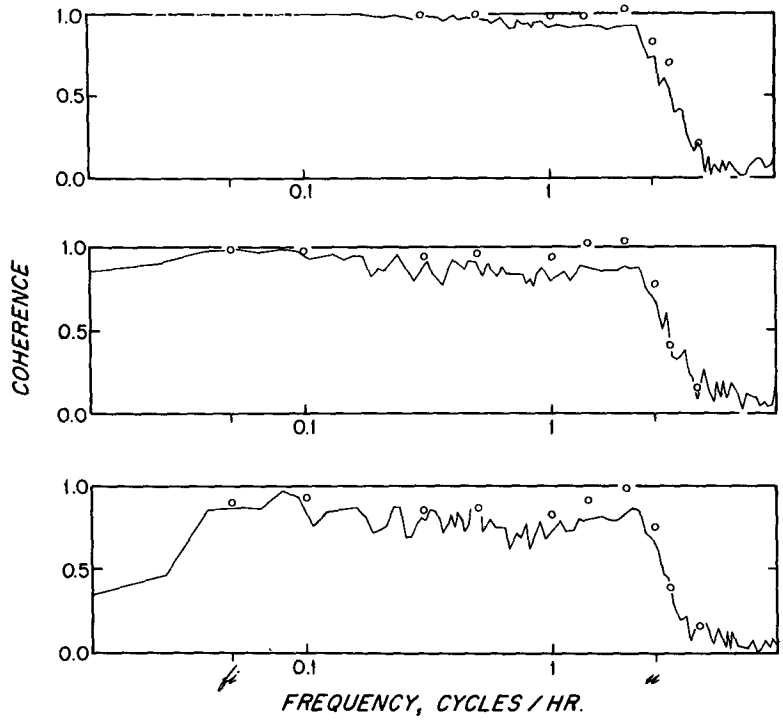

FIG. 6. Observed coherence of temperature fluctuations for separations $Y=2.1$, 7.0 and 28.9 m (top to bottom). Sample points using Eq. (40) in text are indicated. They represent "uncontaminated" internal wave measurements. Modeled coherences in excess of 1 are due to statistical fluctuations in the data and would be absent with increased degrees of freedom.

(12b)] is estimated from (37) and (6):

$$r=\frac{\beta}{2\sqrt{\pi\alpha^2 Z}}\sqrt{\frac{f}{f_i}}=1.21\times10^{-1}\sqrt{f}\,[\text{cph}]^{-\frac{1}{2}}, \quad (41)$$

where f_i is the inertial frequency (0.04 cph). The modulus of $\bar{C}_{ij}^{T}$ given by (40) is shown in Fig. 6 as circled points for three different separations. In each case the internal wave coherence is higher than the temperature coherence, it is more nearly constant over most of the frequency range, and it shows an increase near the buoyancy frequency before dropping

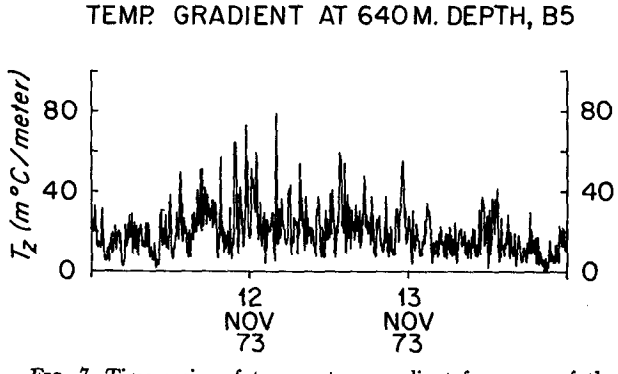

FIG. 7. Time series of temperature gradient from one of the IWEX differential temperature sensors. Note the similarity with Fig. 2.

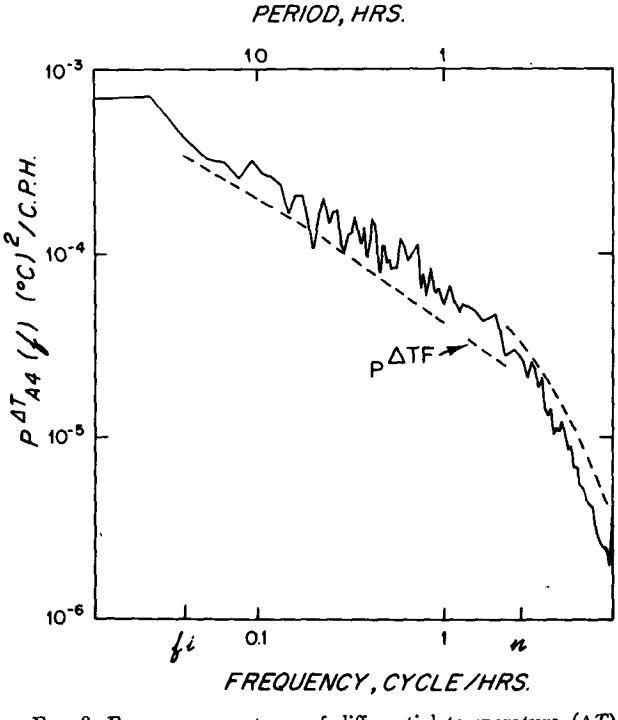

FIG. 8. Frequency spectrum of differential temperature (ΔT) time series with 26 degrees of freedom. Also shown is the model spectrum as described in text.

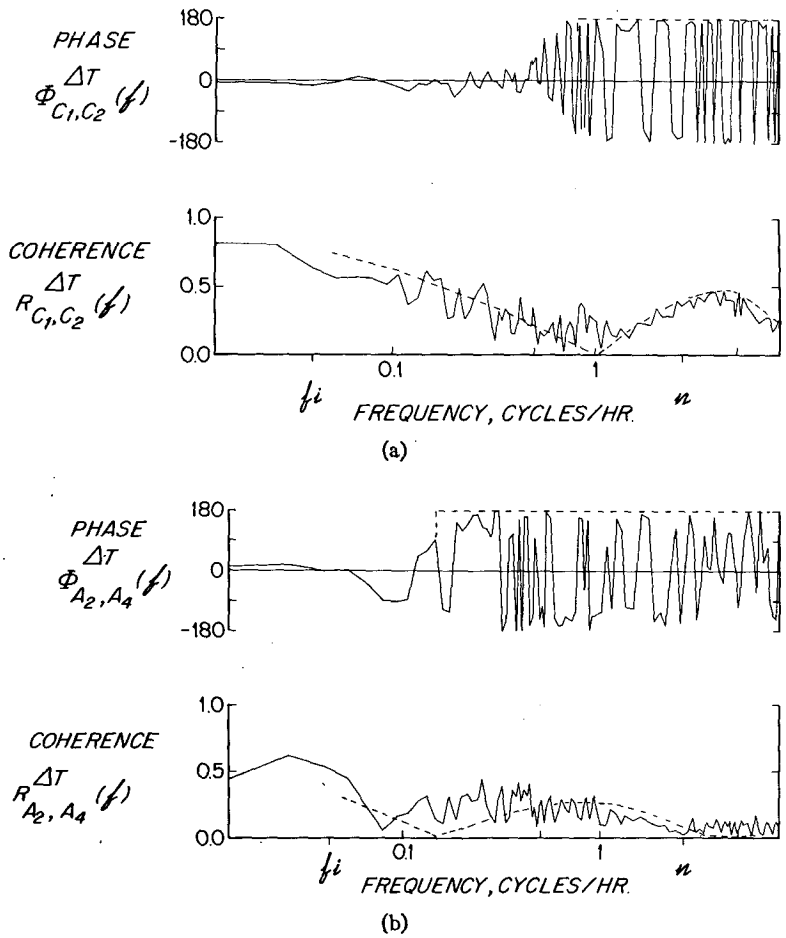

FIG. 9. Observed and modeled vertical coherence and phase for ΔT series (a) $Y=2.1$ m, (b) $Y=4.9$ m. The dashed lines are model results.

off. These features conform to what we expect for internal waves (Garrett and Munk 1975; Cairns and Williams 1976; Desaubies, 1975, 1976).

Note that as the separation increases $C^{TF} \to 0$ rapidly and $\tilde{C}_U^T = R_U^T(1+r)$; the loss of coherence due to finestructure is than given by $(1+r)^{-1}$ and reaches a value of 10 to 15%. For separations in excess of the rms displacement Z, the finestructure field acts as incoherent "noise."

7. The temperature difference measurements

In Fig. 7 we show an example of an ΔT time series from IWEX; it looks quite similar to vertical profiles of temperature gradient (Fig. 2). The power spectrum of this time series is plotted on Fig. 8. In the internal wave band the slope is close to $-\frac{1}{2}$ and beyond the buoyancy frequency it is -2.

The model prediction for the spectrum is given by (18), the second term, $2P^{TF}(1-C^{TF})$, is shown on Fig. 8; it is related to the finestructure. The first term $2\tilde{P}^T(1-\tilde{C}^T)$ represents the straining of the mean gradient by the internal wave field, thus contributing to the fluctuations in the temperature difference signal ΔT. If the wave field was perfectly coherent over $\Delta = 1.74$ m, $\tilde{C}^T = 1$, this contribution would vanish. However, even though $\tilde{C}^T$ is close to 1 (probably >0.99), the first term cannot be discarded *a priori;* this is because $\tilde{P}^T$ is so much larger than $P^{\Delta T}$ (two or three orders of magnitude) that the product $2\tilde{P}^T(1-C^T)$ can be of the order of $P^{\Delta T}$, and is very sensitive to the value of $\tilde{C}^T$ as well as its frequency dependence. Present internal wave models already referenced purport that $\tilde{C}^T$ is independent of frequency; thus any internal wave contribution to $P^{\Delta T}(f)$ would have a slope of -2. It appears from Fig. 8 that the finestructure term accounts for most, but not all, of the variance in the ΔT signal for $f<n$ and overestimates the spectral level for $f>n$.

The vertical coherence $R^{\Delta T}$ as given by (21) is plotted in Fig. 9 with $Y=2.1$ and 4.9 m, $\Delta=1.74$ m. The prediction of the model is quite satisfactory; note in particular the change in phase from 0 to $\pm 180°$, and the significant coherence for $f>n$. This effect is definitely related to the finestructure and cannot be accounted for by the internal wave field.

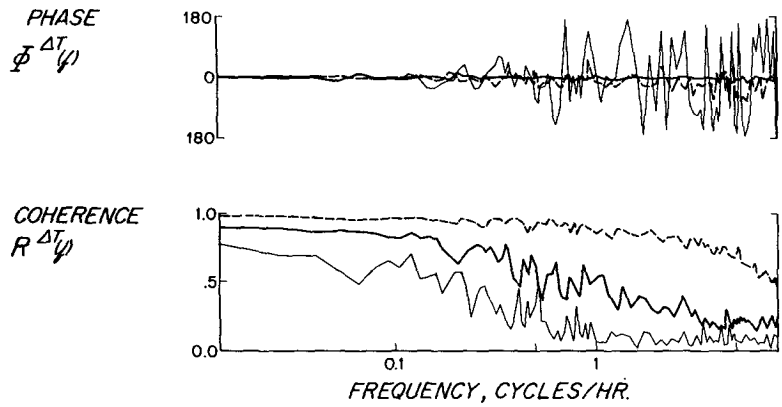

FIG. 10. Observed coherence and phase for ΔT measurements separated horizontally by 14 m (dashed), 44 m (heavy black) and 130 m.

As the vertical separation Y of the sensor pairs increases, the coherence decreases rapidly.

Our model, which does not include any horizontal structure, cannot explain the observed coherence for ΔT sensors horizontally separated. Fig. 10 shows horizontal ΔT coherences with separations of 14, 44 and 139 m. For the smallest separation the coherence is high at all frequencies, even beyond n. The corresponding temperature coherences are uniformly higher than the ΔT coherences. We infer that Fig. 10 reflects the horizontal structure of the layered structure. The significant loss of coherence for larger separations suggests that there exist inhomogeneities of that horizontal scale.

Finally we note that in the presence of internal waves, regions of high temperature (density) gradient are also regions of high velocity shear, corresponding to "velocity finestructure." The modeling of this field is underway and could be relevant to the observed differences between moored temperature/velocity coherences noted by Briscoe (1975).

8. The dropped temperature measurements

The original vertical series were used to obtain the finestructure parameters rather than the vertical spectra. In Section 2 a model spectrum was derived which included a wave-like and a step-like component. We will now compare the measured/modeled spectra. In Fig. 11 the temperature spectrum observed in the main thermocline by Hayes (1975) is compared with the spectrum from (28), which purports to model the finestructure for vertical scales larger than $Z \approx 7$ m.

As discussed in Section 2, following (24) the vertical spectra are the sum of two contributions: a finestructure spectrum given by (28), and an internal wave spectrum. The finestructure spectrum contributes about one-half of the variance to the total observed spectrum (Hayes, 1975) for the region as is shown in Fig. 11.

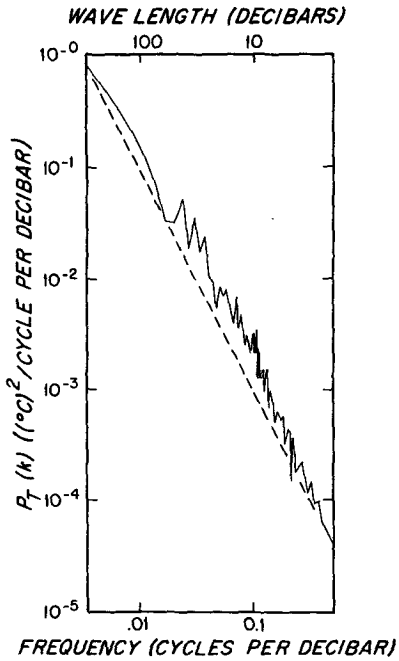

FIG. 11. Vertical wavenumber spectrum of temperature in the main thermocline and modeled finestructure contribution. The latter is only formally correct for wavelengths in excess of $Z \approx 7$ m. See text for details.

9. Conclusions

We have investigated the possibility of discriminating between internal waves and finestructure in moored and dropped temperature measurements. The basic model, involving a Gaussian statistic of the displacement field and a Poisson model for the finestructure, is that of Garrett and Munk (1971) and McKean (1974). It has been extended to describe vertical temperature spectra and the temperature difference measurements of IWEX, with emphasis on accurate estimation of the model parameters and on quantitative predictions.

We find that for the data considered the contamination of moored temperature spectra by finestructure is small, of the order of 10% for low frequencies. However, at high frequencies the effect becomes comparatively more important. A more significant effect is the loss of measured coherence, which increases with frequency and finestructure level; the loss can be of the order of 20% near the buoyancy frequency. This reaffirms our original assumption that internal wave parameters could be obtained from moored measurements (i.e., finestructure contributions are relatively small). The dropped spectra indicate that both internal waves and finestructure contribute about equally to the variability on scales of 10–300 m. This is somewhat disturbing and may indicate that some of our finestructure parameters may be contaminated by waves.

The moored temperature difference measured over a small distance (small with respect to the correlation length of the internal wave field) has been shown to provide a critical check of the model, since this signal is directly related to the finestructure variability. This opens the possibility of using the ΔT measurements as "moored finestructure" time series; one could thus monitor the time variability of the finestructure level intensity and relate it to larger scale phenomena.

Acknowledgments. We wish to acknowledge the assistance of the buoy and CTD groups at the Woods Hole Oceanographic Institution who played a major role in obtaining the IWEX and CTD data. This research was supported by the Applied Physics Laboratory of The Johns Hopkins University, Contract 372111, and the Office of Naval Research via Contract N00014-74-C-0262 NR 083-004.

REFERENCES

Briscoe, Melbourne G., 1975: Preliminary results from the trimoored internal wave experiment (IWEX). *J. Geophys. Res.*, **80**, 3872–3884.

Cairns, J. L., and G. O. Williams, 1976: Internal wave observations from a midwater float. Part II. *J. Geophys. Res.*, **81**, 1943–1949.

Desaubies, Y. J. F., 1975: A linear theory of internal wave spectra and coherences near the Väisälä frequency. *J. Geophys. Res.*, **80**, 895–899.

——, 1976: Analytical representation of internal wave spectra. *J. Phys. Oceanogr.*, **6**, 976–981.

Garrett, C., and W. Munk, 1971: Internal wave spectra in the presence of finestructure. *J. Phys. Oceanogr.*, **1**, 196–202.

——, and ——, 1975: Space-time scales of internal waves—a progress report. *J. Geophys. Res.*, **80**, 291–297.

Gregg, M. C., 1975: Microstructure and intrusions in the California current. *J. Phys. Oceanogr.*, **5**, 253–278.

Hayes, S. P., 1975: Preliminary measurements of time-lagged coherence of vertical temperarure profiles. *J. Geophys. Res.*, **80**, 307–311.

——, T. M. Joyce and R. C. Millard, Jr., 1975: Measurements of vertical finestructure in the Sargasso Sea. *J. Geophys. Res.*, **80**, 314–319.

Joyce, Terrence M., 1976: Large-scale variations of small-scale temperature/salinity finestructure in the main thermocline of the northwest Atlantic. *Deep-Sea Res.* (in press).

McKean, R. S., 1974: Interpretation of internal wave measurements in the presence of finestructure. *J. Phys. Oceanogr.*, **4**, 200–213.

Phillips, O. M., 1971: On Spectra Measured in an undulating layered medium. *J. Phys. Oceanogr.*, **1**, 1–6.

Reid, R. O., 1971: A special case of Phillips' general theory of sampling statistics for a layered medium. *J. Phys. Oceanogr.*, **1**, 61–62.